Nov 4th, 12:00 AM - Nov 5th, 12:00 AM

Experimental Investigation of Distortional Buckling of Cold-Formed Stainless Steel Sections

Maura Leece

Kim J. R. Rasmussen

Seventeenth International Specialty Conference on Cold-Formed Steel Structures
Orlando, Florida, U.S.A, November 4-5, 2004

EXPERIMENTAL INVESTIGATION OF DISTORTIONAL BUCKLING OF COLD-FORMED STAINLESS STEEL SECTIONS

Maura Lecce[1], Kim Rasmussen[2]

Abstract

This paper describes the experimental investigation of the distortional buckling of thin-walled stainless steel sections in compression. Austenitic 304, ferritic 430 stainless steel and ferritic-like 3Cr12 chromium weldable steel sheets were brake-pressed into simple-lipped channels and simple-lipped channels with intermediate stiffeners. A comprehensive procedure to determine the mechanical properties of stainless steel material is described. A total of 19 distortional tests failed at stresses greater than the proportionality stress, and hence were influenced by material non-linearity. Data required to assess current design guidelines in place for distortional buckling of stainless steel compression members are provided herein.

Introduction

Carbon steel is usually the economical choice of building material compared to stainless steel. However, for environmentally sensitive structures, stainless steel offers a clean, long-life and aesthetically pleasing alternative. Stainless steel may also be the preferred material in corrosive environments and compared to unprotected carbon steel, stainless steel has a better fire resistance rating. Whether chosen for functional or aesthetic purposes, the design of stainless steel structures is often modeled after carbon steel, simply because there has been a lack of data available on the behavior of stainless steel structures. However, stainless steel exhibits a non-linear stress strain curve with a low proportionality

[1] PhD Candidate, Department of Civil Engineering, University of Sydney, NSW, Australia
[2] A/Prof., Department of Civil Engineering, University of Sydney, NSW, Australia

stress and loss of material stiffness beyond this stress. Other material characteristics exhibited by stainless steel include different properties in tension and compression, significant work hardening capability and anisotropy. Each of these characteristics depends on the alloy and the history of cold-working and/or annealing. Currently, there is limited data for the distortional buckling failure mode and strength of stainless steel members and consequently a lack of design guidance which considers all material characteristics. The current design procedures in place for distortional buckling refer to those for cold-formed carbon steel. In some cases, this may lead to unconservative designs for stainless steel. Van den Berg (2000) and Buitendag and van den Berg (1994) who conducted research on partially stiffened zed and hat sections made from 304, 430 and 3Cr12 stainless steels, proposed the use of a plasticity reduction factor (E_s/E_o) to account for stress-strain non-linearity and low proportionality stress. The use of plasticity reduction factors, however, leads to iterative design calculations and may not be ideal for designers. This experimental investigation involves austenitic 304, chromium weldable 3Cr12 steel (with properties similar to those of ferritic alloys) alloys, and ferritic 430 alloy, which is less commonly used (AS/NZS 4673 2001). The nominal thicknesses are 2.0mm for the 304 and 3Cr12 material and 1.2mm for the 430 material. Simple lipped channels and lipped channels with intermediate stiffeners were designed and fabricated for this experimental program. Experimental data presented here are also used in a companion paper (Lecce and Rasmussen 2004) to evaluate current design guidelines available in Australian/New Zealand, North American and European standards.

Experimental Investigation

Material Properties

The material investigation of the different stainless steel alloys used was essential for the design of suitable sections and to assess the structural behaviour of the sections tested. Data of particular interest were the strengths in tension and compression, strength enhancement due to work hardening and material anisotropy. These characteristics were determined by: i) tension and compression coupon tests of the flat sheet material in directions longitudinal, transverse and diagonal (45°) to the direction of rolling; ii) tension and

compression corner coupon tests of brake pressed material, tested parallel to the direction of rolling. All coupons were tested in a 300kN capacity MTS Sintech 65/G displacement controlled machine, except for the tensile corner coupons which were tested in a 100kN capacity MTS 810 material testing machine. 304 and 3Cr12 coupons were tested at a strain rate of 0.1mm/min and 430 coupons were tested at 0.05mm/min. The static ultimate load was obtained by halting the machine cross-head displacement.

Flat tensile coupons were made according to specifications in AS 1391 (1991). For flat compression coupons, a special jig which provided continuous support along the coupon length to prevent buckling was used. Compression coupons were approximately 2mm longer than the jig which, when tested was enough to provide a stress strain curve up to 2% strain. Results from tensile and compression coupon tests of the flat material, tested in the longitudinal direction (direction of rolling) are given in Table 1. Ramberg-Osgood parameters, used to define stress-strain non-linearity, including 0.01% proportionality yield stress, $f_{p,f}$, and the 0.2% proof stress, $f_{y,f}$, the n-parameter, and initial elastic modulus E_o are provided. The stresses reported are the dynamic test values. It is important to note here that the Ramberg-Osgood curve used to describe non-linearity produces a stress-strain curve sufficiently accurate up to and slightly beyond the 0.2% proof stress, f_y, but are inaccurate if extrapolated any further. This is a concern particularly for numerical analysis of plates which may obtain high strains at ultimate (Rasmussen 2001). A detailed discussion about constructing the full stress strain curve from Ramberg-Osgood parameters is given in Rasmussen (2001).

Table 1. Flat sheet tension and compression coupon results

Alloy	Load direction	$f_{p,f}$	$f_{y,f}$	n	f_u	Elong.	E_o	Anisotropy ratios calculated at $f_{y,f}$		
		MPa	MPa		MPa	%	GPa	L/L	T/L	D/L
304	LT	138	251	5	703	76	193	1.00	1.02	1.01
304	LC	164	242	8	n/a	n/a	187	1.00	1.05	1.01
430	LT	190	291	7	451	34	185	1.00	1.05	1.08
430	LC	170	271	6	n/a	n/a	193	1.00	1.11	1.09
3Cr12	LT	215	338	7	483	37	195	1.00	1.14	1.09
3Cr12	LC	234	339	8	n/a	n/a	208	1.00	1.14	1.09

Notes: LT=longitudinal tension; LC=longitudinal compression;
L/L=longitudinal/longitudinal stress ratio; T/L=transverse/longitudinal stress ratio;
D/L=diagonal/longitudinal stress ratio; 1 ksi = 6.89 MPa

Table 1 clearly shows that the material properties in tension and compression are not identical. For example, $f_{p,f}$ for alloy 304 in longitudinal tension (LT) is 15.9% greater than $f_{p,f}$ in longitudinal compression (LC) and $f_{y,f}$ (LT) is 4.1% greater than $f_{y,f}$ (LC). The difference in strength is alloy and direction-dependent. Material properties in the transverse and diagonal directions are not detailed, but anisotropy ratios are given for tension and compression tests. As can be seen in Table 1, the transverse/longitudinal (T/L) stress ratios are between 1.02 and 1.14, showing that $f_{y,f}$ in the transverse direction (for both tension and compression) are greater than those in the longitudinal direction. A significant difference also lies in the percentage elongation; the austenitic 304 alloy has an elongation of 76% compared to ferritic alloys 430 and 3Cr12 which have an elongation of 34% and 37% (similar to mild carbon steel), respectively.

Corner coupon test results are given in Table 2. Tensile corner coupons were cut from brake pressed sections. The tested portion was limited to the corner radius. Strain gauges were placed on the inner and outer radius (at the centre) of the tested portion. The coupon ends were flattened and tested under tensile loading. Due to the eccentricity of the strain gauges with respect to the centroid, the modulus of elasticity was very low indicating it was most likely affected by initial bending. The initial modulus of elasticity was particularly low (170GPa) for the thicker material 304 and 3Cr12, which also had a larger corner radius compared to the thinner 430 material (see Table 2). A jig for the corner compression coupon tests was designed, similar to that used for flat coupon compression tests, except the jig was machined to cradle the outer corner radius exactly (corners of 304 and 3Cr12 tested only). Small 2mm strain gauges were placed on the thickness of the corner coupons at mid-height. An internal rod, with a radius matching the inner radius of the corner coupon, was placed between two identical corner coupons tested simultaneously. Ramberg-Osgood parameters are also given in Table 2. These tests were not affected by initial bending and the initial modulus is more reliable.

Table 2. Corner tension and compression coupon results

Stainless steel alloy	Load Direction	$f_{p,c}$ MPa	$f_{y,c}$ MPa	n	E_o GPa
304	LT	300	570	5	(170)
304	LC	276	565	4	205
430	LT	326	452	9	(195)
430	LC	n/a	n/a	n/a	n/a
3Cr12	LT	425	544	13	(170)
3Cr12	LC	410	606	8	211
Notes: LT=longitudinal tension; LC=longitudinal compression; 1 ksi = 6.89 MPa					

Stainless steel is greatly affected by cold-working and the strength enhancement at the corners of a brake pressed section cannot be ignored in numerical analysis. This is particularly true for austenitic stainless steels, such as the 304 material used in this program, which have face-centred crystal structure. Ferritic alloys such as 430 and 3Cr12 have a body centred crystal structure and are less affected by cold-working (Rasmussen et al. 2003). For instance, the corner $f_{y,c}$ (LC) for austenitic alloy 304 is 2.33 times larger than the flat $f_{y,f}$ (LC) (see Tables 1 and 2). This is consistent with Rasmussen et al. (2003) who found that for annealed plates which have been brake pressed, the cold-working in the corners can result in a proof stress greater than 2 times the annealed (or virgin) material. Results obtained here are comparable to those obtained by van den Berg and van der Merwe (1992).

Experimental Rationale: Distortional Buckling Section Design

A finite strip elastic buckling analysis, Thin Wall (Papangelis and Hancock 1995), was used to aid in the design of suitable cross sections for distortional buckling. Sections for which the elastic buckling stress was greater than the proportionality stress were chosen so that the effects of non-linearity can be captured in the tests. Thin Wall analysis provides the elastic buckling stress versus buckling half-wave length plot for a cross section assuming simply supported ends. As such, a spline analysis, which can incorporate fixed end conditions, was also used. Figure 1 shows the results of a finite strip and spline finite strip analysis for a simple lipped channel of 304. These two plots clearly show that end conditions and column length influence the distortional elastic buckling stress. Unlike the spline analysis, Thin Wall produces a plot with two distinct minima to represent local buckling and distortional buckling and finally an asymptotic portion representing overall buckling (left to right on Figure 1). From these two plots, a section geometry and length were chosen. Simple lipped channels and lipped channels with intermediate stiffeners in the flanges and web were chosen for each alloy. The cross-sections chosen are shown schematically in Figure 2. Intermediate stiffeners for all specimens were placed at the centre of the web and flanges and had a nominal width of 20mm and depth of 10mm (see Figure 2).

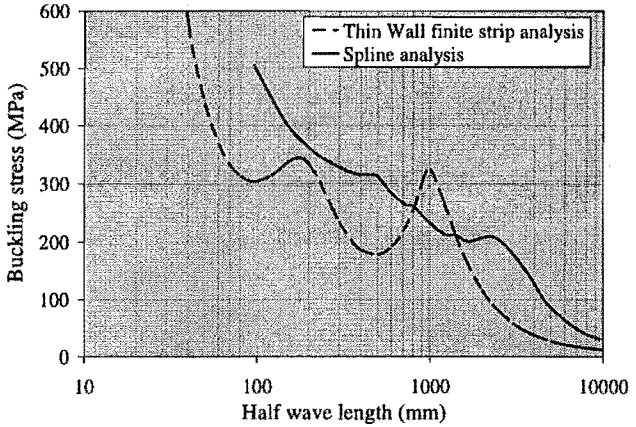

Figure 1. Thin Wall finite strip and spline finite strip analyses

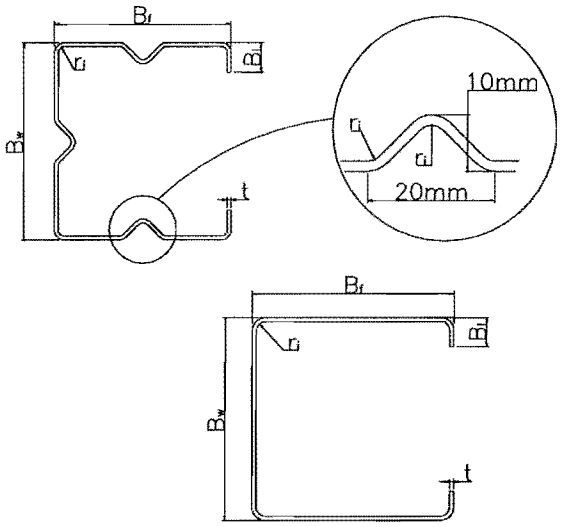

Figure 2. Schematic of lipped channel with intermediate stiffeners and simple lipped channel

Stub Column Tests

A 300kN capacity MTS Sintech 65/G displacement controlled testing machine was used for stub column tests. Typically, two tests were performed for each section (with the exception of section 430D2). Sections were made to lengths in accordance with the recommendations in Galambos (1998) between 3d and 20r, where d is the web depth and r is the least radius of gyration. The ends were machined flat to obtain uniform compression. The gross area was determined by measuring the stub column mass and length and back calculating from the density. Vertical displacement was measured using two LVDTs mounted on either side of the stub column along the weak centroidal axis. The average of the two LVDT readings gave the displacement of the centroid of the section. Two 5mm rods were fed through 5.5mm diameter holes drilled at a distance of 15mm or 20mm from the stub column ends. The hole clearance of approximately 0.5mm allowed any rotation of the section to occur without bending the rods. Elastics were wrapped around the top and bottom rods on either side of the stub column to ensure that the rods did not move during testing. The stub columns were fixed in pattern stone forms on both ends and 4 to 8 strain gauges were placed at mid length around the cross section to monitor alignment and strains. The stub column set up is shown in Figure 3. After the stub column was centred in the testing machine, the machine cross-head was lowered and a small load was applied to keep the specimen in place while the spherical base was allowed to rotate so that the specimen was flush at both the top and bottom, and subsequently locked in place. A constant displacement rate of 0.1mm/min for the thicker 3Cr12 and 304 material (t = 1.98mm and 1.96mm, respectively) and 0.05mm/min for the thinner 430 material (t = 1.13mm) was used (identical to coupon test strain rates). The static ultimate stub column load was determined by halting the testing machine at the peak load for two minutes. However, to be consistent with reported coupon test values the average stub column dynamic ultimate loads, $P_{u,sc}$, are listed in Tables 3 and 4.

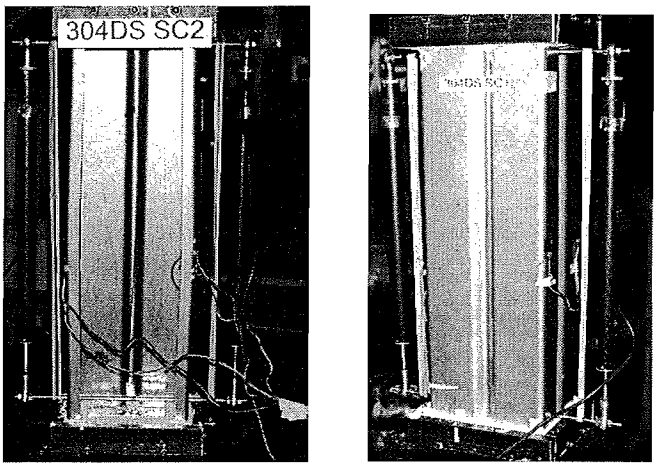

Figure 3. Stub column test set up

Imperfections

Initial imperfection data is essential to develop correct initial conditions for future numerical investigations. Imperfections were measured using calibrated lasers. For the simple lipped channels, imperfections were taken along parallel lines 5-10mm from each corner and along the middle of each element. For channels with intermediate stiffeners, measurements were taken along parallel lines at 5-10mm from each corner. The lasers, displaced by a stepping motor, were programmed to take readings approximately every 2mm along the length of the specimen. Typically more than 1000 readings were taken per line. Two sets of readings were taken for each line measured. Due to space limitations, imperfection values are not presented here but for example, the average maximum imperfection value for the 304D series tests is 0.25mm.

Distortional Buckling Tests

The 300kN capacity MTS Sintech 65/G displacement controlled testing machine was also used for distortional buckling tests. The set up procedures were identical to those used for stub columns except strain gauges and vertical LVDTs were not used. Typically, twin specimens were tested to ensure repeatability of tests and to confirm that set up procedures were consistent. Between 12 and 15 LVDTs were placed around the specimen to monitor lateral movement of the flanges and web. At least four LVDTs were placed at the

corners of the specimen, at approximately mid-length to monitor rotations and overall movement. Other LVDTs were set up at the flange-lip corner and mid point of the web. Figure 4 shows the test set up. Tables 3 and 4 show the results for simple lipped channels and lipped channels with intermediate stiffeners, respectively. Static ultimate loads were obtained by halting the testing machine near peak load. However, the dynamic ultimate loads, P_u, are reported here. The specimen identification used in these tables indicates the alloy used, the cross section type and test number. For example, in Table 3 "304D1a" represents "304" austenitic stainless steel alloy, "D" distortional buckling of simple lipped channel and test number "1a". The twin test specimen for 304D1a is 304D1b. A change in cross section or length is represented by a different test number. The specimen identifications used in Table 4 are similar except "DS" represents distortional buckling of lipped channels with intermediate stiffeners.

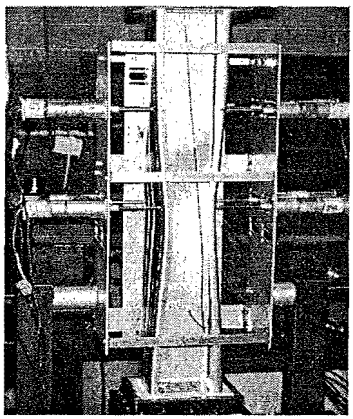

Figure 4. Distortional buckling test set up (304D2a)

Table 3. Measured dimensions and experimental results for simple lipped channels

Specimen ID	L	B_w	B_f	B_l	t	r_i	A_g	P_u	$P_{u,sc}$
	mm	mm	mm	mm	mm	mm	mm^2	kN	kN
304D1a	800	106.3	90.2	12.7	1.96	4.00	565	102	116
304D1b	800	105.8	90.0	12.5	1.96	4.00	565	101	116
304D2a	600	105.5	90.0	12.5	1.96	4.00	565	104	116
304D2b	600	105.6	90.1	12.5	1.96	4.00	565	104	116
430D1a	800	67.9	57.4	8.4	1.13	2.43	211	39	50
430D1b	800	67.7	57.6	8.6	1.13	2.50	211	39	50
430D2	480	67.5	58.5	10.0	1.13	2.50	215	45	n/a
430D3a	780	55.9	54.8	8.6	1.13	2.50	188	40	51
430D3b	782	55.6	54.9	8.7	1.13	2.50	188	39	51
3Cr12D1a	1175	105.0	85.5	14.8	1.98	4.00	555	138	162
3Cr12D1b	1178	105.0	85.4	14.8	1.98	4.00	555	139	162

Notes: 1 in= 25.4 mm; 1 kip= 4.45 kN; P_u= distortional test ultimate load; $P_{u,sc}$=stub column ultimate load

Table 4. Measured dimensions and experimental results for lipped channels with intermediate stiffeners

Specimen ID	L	B_w	B_f	B_l	t	r_i	A_g	P_u	$P_{u,sc}$
	mm	mm	mm	mm	mm	mm	mm^2	kN	kN
304DS1a	788	122.1	90.6	15.0	1.96	3.00	634	132	163
304DS1b	785	122.2	90.6	15.0	1.96	3.00	634	134	163
430DS1	875	79.6	70.0	10.5	1.13	2.50	269	60	81
430DS2	600	79.5	70.2	10.7	1.13	2.50	269	62	81
430DS3	879	79.6	70.3	14.3	1.13	2.50	278	64	88
430DS4	600	79.5	70.7	14.2	1.13	2.50	278	72	88
3Cr12DS1a	1175	110.7	75.5	15.0	1.98	3.00	565	163	198
3Cr12DS1b	1176	111.1	75.7	15.0	1.98	3.00	565	161	198

Notes: 1 in=25.4 mm; 1 kip=4.45 kN; P_u= distortional test ultimate load; $P_{u,sc}$=stub column ultimate load

Discussion and Analysis of Results

All tests except for 430D2 failed by distortional buckling. 430D2 showed signs of local and distortional buckling interaction, with local buckling occurring at a lower load than distortional buckling. Repeatability of ultimate load was established within 2%, confirming reliability of testing procedures. The post-ultimate behaviour, however was not necessarily identical. For example, specimen 304DS1a and 304DS1b, which have the same nominal cross section dimensions and length obtained essentially the same ultimate load (see Table 4) but behaved differently. Both tests produced the same number of distortional buckling half-waves (2) but the flanges of specimen 304DS1a moved in towards the geometric centroid of the section whereas the flanges of specimen 304DS1b moved away from the centroid. The latter maintained the ultimate load over a greater vertical displacement, thus producing a more ductile failure. The load versus stroke graph is shown in Figure 5.

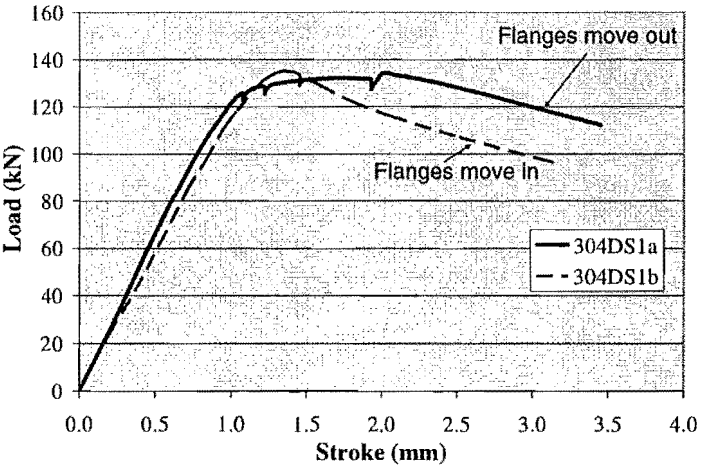

Figure 5. Load versus stroke for 304DS1a and 304DS1b

Whether flanges move towards the centroid or away from the centroid may be influenced by imperfections and this warrants further examination in numerical analysis. Prola and Camotim (2002) investigated the post-buckling behaviour of cold-formed lipped channel sections made from conventional carbon steel and

found that the distortional post buckling strength of a section where flanges move towards each other is higher than if flanges move away from each other. They concluded that the difference can be attributed to the difference in the warping restraint present in the flanges and lips. This result is at odds with the results shown in Figure 5. From an ultimate limit states design perspective, however, the results shown here suggest that the post ultimate behaviour is not as critical as the ultimate capacity.

Another important observation can be made from Table 4, by comparing the test results of 430DS1, 430DS2, 430DS3 and 430DS4. The cross section dimensions are nominally the same except for the lip width, where 430DS1 and 430DS2 have a lip width of 10mm and 430DS1 and 430DS2 have a lip width of 14mm. For 430DS1 and 430DS2, an increase in length of approximately 280mm resulted in a decrease in ultimate load of 2kN and for 430DS3 and 430DS4, an increase in length of approximately 280mm resulted in a decrease in ultimate load of 8kN. Specimens 430DS1 and 430DS2 (B_l=10mm), therefore are not as sensitive to changes in length. For the same length of 600mm, a 3% increase in gross sectional area produces approximately 16% increase in strength (compare 430DS2 and 430DS4). Finite element analysis is required to investigate the effectiveness of different lip sizes and their influence on ultimate strength.

The experimental average peak stress (ultimate load divided by gross area) is greater than the proportionality stress for all test specimens. Using average ultimate stresses (P_u/A_g) and Ramberg-Osgood stress strain parameters based on longitudinal compression of flat material, the tangent and secant moduli, E_t and E_s, were evaluated. E_t and E_s are given by the following equations (AS/NZS 4673 2001),

$$E_t = \frac{f_y E_o}{f_y + 0.002 n E_o \left(\frac{f}{f_y}\right)^{n-1}} \qquad E_s = \frac{E_o}{1 + 0.002 E_o \left(\frac{f^{n-1}}{f_y^n}\right)}$$

In the above equations $f = (P_u/A_g)$. These calculations are shown in Tables 5 and 6 for simple lipped channels and lipped channels with intermediate stiffeners, respectively.

Table 5. Tangent and secant moduli for simple lipped channels calculated at the mean ultimate stress

Specimen ID	Experimental data				Ramberg-Osgood parameters of flat material				Tangent and secant moduli			
	L	A_g	P_u	P_u/A_g	$f_{p,f}$	$f_{y,f}$	E_o	n	E_t	E_t/E_o	E_s	E_s/E_o
	mm	mm^2	kN	MPa	MPa	MPa	GPa		GPa		GPa	
304D1a	800	565	102	181	164	242	187	8	72	0.39	156	0.83
304D1b	800	565	101	179	164	242	187	8	75	0.40	158	0.84
304D2a	600	565	104	184	164	242	187	8	66	0.35	152	0.81
304D2b	600	565	104	184	164	242	187	8	66	0.35	152	0.81
430D1a	800	211	39	182	170	271	193	6	88	0.46	161	0.84
430D1b	800	211	39	185	170	271	193	6	85	0.44	159	0.83
430D2	480	215	45	209	170	271	193	6	58	0.30	139	0.72
430D3a	780	188	40	211	170	271	193	6	56	0.29	137	0.71
430D3b	782	188	39	206	170	271	193	6	61	0.32	142	0.74
3Cr12D1a	1175	555	138	249	234	339	208	8	98	0.47	182	0.88
3Cr12D1b	1178	555	139	251	234	339	208	8	95	0.46	181	0.87
Notes: 1 in = 25.4 mm; 1 kip = 4.45 kN; 1 ksi = 6.89 MPa												

Table 6. Tangent and secant moduli for lipped channels with intermediate stiffeners calculated at the mean ultimate stress

Specimen ID	Experimental data				Ramberg-Osgood parameters of flat material				Tangent and secant moduli			
	L	A_g	P_u	P_u/A_g	$f_{p,f}$	$f_{y,f}$	E_o	n	E_t	E_t/E_o	E_s	E_s/E_o
	mm	mm^2	kN	MPa	MPa	MPa	GPa		GPa		GPa	
304DS1a	788	634	132	208	164	242	187	8	35	0.19	121	0.65
304DS1b	785	634	134	211	164	242	187	8	32	0.17	117	0.63
430DS1	875	269	60	222	170	271	193	6	47	0.24	127	0.66
430DS2	875	269	62	230	170	271	193	6	41	0.21	119	0.62
430DS3	600	278	64	228	170	271	193	6	42	0.22	120	0.62
430DS4	879	278	73	258	170	271	193	6	25	0.13	91	0.47
3Cr12DS1a	1175	565	163	288	234	339	208	8	50	0.24	149	0.72
3Cr12DS1b	1176	565	161	285	234	339	208	8	53	0.26	153	0.73
Notes: 1 in = 25.4 mm; 1 kip = 4.45 kN; 1 ksi = 6.89 MPa												

For simple lipped channels, E_t/E_o ranges from 0.29 to 0.47 and E_s/E_o ranges from 0.71 to 0.88. For lipped channels with intermediate stiffeners E_t/E_o ranges from 0.13 to 0.26 and E_s/E_o ranges from 0.47 to 0.73. This clearly shows that distortional buckling occurred in the non-linear range of the stress strain curve. Van den Berg (2000) also found that partially stiffened stainless steel hat and zed sections loaded in compression exhibited inelastic behaviour. This loss in

stiffness is an important consideration in the development of design guidelines for the distortional buckling of stainless steel.

Conclusions

This paper describes the experimental procedures used for testing distortional buckling of simple lipped channels and lipped channels with intermediate stiffeners for austenitic 304, ferritic 430 and ferritic-like 3Cr12 (chromium weldable steel) stainless steel alloys. Material properties vary with each alloy and they depend on the direction of loading. The strength enhancement due to work hardening in the brake-pressed corners is particularly pronounced for the austenitic 304 alloy, with a proof stress 2.33 times larger than the flat sheet material. Non-linear stress strain behaviour with a markedly low proportionality stress leads to a significant loss of stiffness at low loads and this is reflected in the test results. A total of 19 distortional buckling tests are presented and data are now available to evaluate current design guidelines. Further investigations using finite element analysis are required to examine the influence of stainless steel material characteristics, imperfections, cross section slenderness and column length on the distortional buckling behaviour.

Appendix – Notation

A_g	gross area
B_f	overall flange width
B_l	overall lip width
B_w	overall web width
d	section depth
D/L	diagonal/longitudinal stress ratio
E_o	initial elastic modulus
E_s	secant modulus
E_t	tangent modulus
f	normal stress
f_p	0.01% proportionality stress
$f_{p,c}$	0.01% proportionality stress of corner (cold-worked) material
$f_{p,f}$	0.01% proportionality stress of flat (virgin) material
f_u	ultimate stress
f_y	0.2% proof stress
$f_{y,c}$	0.2% proof stress of corner (cold-worked) material
$f_{y,f}$	0.2% proof stress of flat (virgin) material
L	column length

LC	longitudinal compression
LT	longitudinal tension
LVDT	linearly varying displacement transducer
L/L	longitudinal/longitudinal stress ratio
n	Ramberg-Osgood parameter
P_u	distortional test ultimate load
$P_{u,sc}$	stub column test ultimate load
r	least radius of gyration
r_i	inner corner radius
t	thickness
T/L	transverse/longitudinal stress ratio

Appendix – References

AS 1391 (1991). *Methods for Tensile Testing of Metals*, Australian Standard 1391:1991, Standards Association of Australia, Sydney, Australia.

AS/NZS 4673 (2001). *Cold-Formed Stainless Steel Structures.* Australian/New Zealand Standards 4673:2001, Standards Australia, Sydney, Australia.

Buitendag, Y., van den Berg, G.J. (1994). *The Strength of Partially Stiffened Stainless Steel Compression Members.* Proceedings of the 12th Specialty Conference on Cold-Formed Steel Structures, St Louis.

Galambos, T.V. (ed.) (1998). *Guide to Stability Design Criteria for Metal Structures.* 5th ed., Wiley & Sons, New York, U.S.A. pp. 814-822. (Technical Memorandum No. 3 of the Structural Stability Research Council: Stub Column Test Procedures).

Lecce, M., and Rasmussen, K.J.R. (2004). *Design of Stainless Steel Against Distortional Buckling.* Proceedings of the 17th International Conference on Cold-Formed Steel Structures, Orlando.

Papangelis, J.P. and Hancock, G.J. (1995). *Computer Analysis of Thin- Walled Structural Members.* Computers and Structures, 56(1), pp. 157-176.

Prola, L.C., and Camotim, D. (2002). *On the Distortional Buckling of Cold-Formed Lipped Channel Steel Columns.* Proceedings of SSRC 2002 Annual Stability Conference, pp. 571-590.

Rasmussen, K.J.R. (2001). *Full-range Stress-Strain Curves for Stainless Steel Alloys.* Journal of Constructional Steel Research, 59(1), pp. 47-61.

Rasmussen, K.J.R., Burns, T., Bezkorovainy, P., Bambach, M. (2003). *Numerical Modelling of Anisotropic Stainless Steel Plates.* Journal of Constructional Steel Research, 59(11), pp. 47-61.

van den Berg, G.J., van der Merwe, P. (1992). *Prediction of Corner Mechanical Properties for Stainless Steels Due to Cold-Forming*. Proceedings of the 11th Specialty Conference on Cold-Formed Steel Structures, St. Louis.

van den Berg, G.J. (2000). *The Effect of the Non-Linear Stress-Strain Behaviour of Stainless Steels on Member Capacity.* Journal of Constructional Steel Research, 54(1), pp. 135-160.